

Report

Preferential Occurrence of Chromosome Breakpoints within Early Replicating Regions in Neuroblastoma

Isabelle Janoueix-Lerosey^{1,2}

Philippe Hupé^{3,5}

Zofia Maciorowski⁴

Philippe La Rosa⁵

Gudrun Schleiermacher^{1,2}

Gaëlle Pierron⁶

Stéphane Liva⁵

Emmanuel Barillot²

Olivier Delattre^{1,2,*}

¹Laboratoire de Pathologie Moléculaire des Cancers; ²INSERM, U509; ³UMR 144 CNRS; ⁴Service de Cytométrie; ⁵Service Bioinformatique; ⁶Unité de Génétique Somatique, Institut Curie; Paris, France

*Correspondence to: Olivier Delattre; Institut Curie; INSERM U509; Laboratoire de Pathologie Moléculaire des Cancers; 26 rue d'Ulm; Paris, 75248 France; Tel.: +33.1.42.34.66.79; Fax: +33.1.42.34.66.30; Email: delattre@curie.fr

Received 09/13/05; Accepted 10/14/05

Previously published online as a Cell Cycle E-publication:
<http://www.landesbioscience.com/journals/cc/abstract.php?id=2257>

KEY WORDS

neuroblastoma, replication timing, translocations breakpoints, genomic microarrays

ABBREVIATIONS

AWS	Adaptive Weights Smoothing
BIR	Break-Induced Replication
CGH	Comparative Genomic Hybridisation
Cy3	Cyanin 3
Cy5	Cyanin 5
DSB	Double Strand Break
NB	Neuroblastoma

ACKNOWLEDGEMENTS

We would like to thank Kathryn Woodfine and Nigel Carter from the Wellcome Trust Sanger Institute for providing the last release of their replication timing data. This work was supported by grants from the Ligue Nationale Contre le Cancer (Equipe labellisée). The construction of the 3.3k BAC array was supported by grants from the Carte d'Identité des Tumeurs (CIT) Program of the Ligue Nationale Contre le Cancer.

ABSTRACT

Neuroblastoma (NB) is a frequent paediatric extra cranial solid tumor characterized by the occurrence of unbalanced chromosome translocations, frequently, but not exclusively, involving chromosomes 1 and 17. We have used a 1 Mb resolution BAC array to further refine the mapping of breakpoints in NB cell lines. Replication timing profiles were evaluated in 7 NB cell lines, using DNAs from G₁ and S phases flow sorted nuclei hybridised on the same array. Strikingly, these replication timing profiles were highly similar between the different NB cell lines. Furthermore, a significant level of similarity was also observed between NB cell lines and lymphoblastoid cells. A segmentation analysis using the Adaptive Weights Smoothing procedure was performed to determine regions of coordinate replication. More than 50% of the breakpoints mapped to early replicating regions, which account for 23.7% of the total genome. The breakpoints frequency per 10⁸ bases was therefore 10.84 for early replicating regions, whereas it was only 2.94 for late replicating regions, these difference being highly significant ($p < 10^{-4}$). This strong association was also observed when chromosomes 1 and 17, the two most frequent translocation partners in NB were excluded from the statistical analysis. These results unambiguously establish a link between unbalanced translocations, whose most likely mechanism of occurrence relies on break-induced replication, and early replication of the genome.

INTRODUCTION

Neuroblastoma (NB) is a frequent neoplasm of childhood that derives from primitive cell of the sympathetic nervous system.¹ The specific genetic alterations of NB tumors and cell lines have been explored through a panel of techniques, including Southern blot, FISH, allelotyping, chromosomal CGH (Comparative Genomic Hybridisation) and 24-color or spectral karyotyping.²⁻⁹ Interestingly, these analyses revealed that most rearrangements were unbalanced. At the difference of balanced translocations, which exchange two chromosomal segments, giving rise to two derivative chromosomes without any gain or loss of genetic material, unbalanced translocations replace the distal segment of one chromosome by material from another chromosome. Unbalanced translocations are therefore characterized by the presence of only one derivative chromosome, and result in loss and/or gain of genetic material. Recently, a combined chromosomal CGH and 24-color karyotyping analysis of 27 NB cell confirmed that unbalanced translocations are 10 times more frequent than balanced translocations.⁶ This combined analysis also lead to a low resolution mapping of nonreciprocal translocation breakpoints, revealing that the distribution of chromosome breakpoints was not random but skewed toward certain chromosomes particularly rich in early replicating regions. Recently, a powerful replication timing assay using genomic microarrays that allows quantifying the change in genomic copy number occurring during the S phase of the cell cycle has been described and used to determine the replication profile of a human lymphoblastoid cell line of normal karyotype.¹⁰ In order to more precisely map and compare the positions of breakpoints with respect to replication timing, we now report the use of a genomic array containing 3400 BAC/PAC clones, to explore both the position of the unbalanced translocations breakpoints and the patterns of replication along each chromosome in several NB cell lines. We show that the replication timing profiles are highly similar among different NB cell lines and that a general conservation also exists between NB cell lines and lymphoblastoid cells. We unambiguously establish that unbalanced translocations in NB cell lines occur preferentially in early replicating regions.

MATERIALS AND METHODS

Cell lines culture. NB cell lines (CLB-Ge, GI-M-EN, IMR32, KCNR, SJNB-8, SK-N-AS and SK-N-BE) were grown in DMEM or RPMI-1640 media supplemented with 10% foetal calf serum, as previously described.⁶ Cells were harvested 24–48 hours after division to maximize the proportion of cells in S phase. Cells were centrifuged at 1500 rpm for 5 mins and washed twice with 1x PBS. The pellet was resuspended in 1 ml of 1x PBS and cells were fixed by the addition of 3 ml cold ethanol. Fixed cells were stored at 4°C until stained with propidium iodide for cell sorting.

Flow sorting and DNA extraction. Fixed cells were centrifuged 5 mins at 2800 rpm then resuspended in staining buffer containing 0.05% Tween 80, propidium iodide at 25 µg/ml and RNase at 25 µg/µl. This mixture was incubated 15 min at 37°C just prior to sorting. Stained nuclei were separated into different phases of the cell cycle using a FACSVantage diva SE cell sorter (BD Biosciences). For each cell line, two sorts were performed: in a first experiment, nuclei were sorted into total S and G₁ phase fractions whereas, in a second experiment, nuclei were sorted into S1 (first quarter of the S phase) and S2 (second quarter of the S phase) fractions. Typical ranges of cellular DNA content were 1.24, 1.4 and 1.45 for S1, S2 and total S fractions, respectively. The sorted fractions were checked for purity by analysis on a second sorter (FacsSort, BD Biosciences). To extract DNA, an equal volume of 2x lysis buffer (100 mM Tris pH = 7.5, 100 mM EDTA pH = 8, 2% SDS and 500 µg/µl proteinase K) was added to each fraction and the nuclei were incubated overnight at 50°C. DNA extraction was then performed using standard procedure.

Whole genome amplification. A whole genomic amplification was performed to amplify DNA for S1 fractions of 6 NB cell lines. No amplification was performed for the CLB-Ge cell line since, in that case, a sufficient amount of DNA was obtained from the sorted cells. We used the GenomiPhi DNA Amplification kit containing the Phi29 DNA Polymerase (Amersham Biosciences). 50 ng of genomic DNA were used for amplification, according to the manufacturer's instructions, which led to a yield of approximately 10 µg.

Genomic microarray preparation. Our genome wide arrays contain 3400 PAC/BAC clones spaced at approximately 1 Mb intervals, spotted in triplicate on Ultra Gaps slides (Corning). Chromosomes 1, 17 and 22 exhibit a higher coverage, the number of clones per Mb being 1.8, 2 and 1.5, respectively. Among chromosomes 1 and 17, the regions from 1pTel to 30 Mb on 1p arm and from 27.5 to 37.5 Mb on 17q arm are also covered at a higher density. All clones were validated by ends' sequencing. Precise coordinates of the clones were obtained by BLAT analysis on the May 2004 release of the Human Genome Browser Gateway (HGBG) (<http://genome.ucsc.edu/>).

DNA labelling, hybridisation and array analysis. Random primed labelling with dCTP-Cy3 or dCTP-Cy5 and hybridisations were performed as previously described.¹¹ Images were acquired using a dual laser scanner (Axon 4000B scanner, Axon Instruments). Spots quantification was done with GenePix Pro 5.1 imaging software (Axon Instruments).

Normalization. Normalization was performed using the MANOR algorithm, which enables to correct spatial effects (Neuviel et al manuscript in preparation). In brief, this algorithm proceeds in four steps: (1) estimation of the spatial trend on the background signal of Cy 3 channel using two-dimensional LOESS, (2) segmentation of the array into spatial areas with similar trend values, using the unsupervised classification algorithm NEM (Neighborhood Expectation Maximization) including spatial constraints, (3) definition of areas affected by spatial bias and (4) subtraction of the spatial trend from the log(Cy5/Cy3) values. After this process, clone replicates are averaged.

Statistical analysis

Breakpoint identification. We used the DAGLAD algorithm (Deletion, Amplification, Gain and Loss Analysis of DNA) to identify the breakpoints and genomic alterations in array-CGH profiles (Hupé et al manuscript in preparation). This algorithm is an improvement of the GLAD algorithm (Gain and Loss Analysis of DNA) which has been previously described.¹² This algorithm is based on the Adaptive Weights Smoothing (AWS) procedure

and penalized likelihood. It allows the delineation of regions with similar DNA copy number. A breakpoint corresponds to the transition between two consecutive regions.

Correlation of replication timing data for the various NB samples. For each pair-wise comparison of S/G₁ ratios between two cell lines, a correlation coefficient, r , was calculated. Then, we tested the hypothesis of r being different from 0 using the Student's t-test on the t-statistic = $r \cdot (N - 2)^{1/2} / (1 - r^2)^{1/2}$ with $(N - 2)$ degrees of freedom, N being the sample size.

Determination of replication timing profiles using segmentation analysis. To determine the replication timing profiles, we used the AWS procedure to define piece wise of coordinate replication. For robustness consideration we decided to estimate the piecewise constant function over an averaged profile rather than for each cell line separately. For each profile, the log-ratios were centered on their median. The standard-deviation was estimated based on Inter Quartile Range as previously described¹² and centered profiles were scaled at unit variance then averaged. Finally, the averaged profile was rescaled by the average of the standard-deviation calculated over the set of profiles. The length of regions with coordinate replication is expected to be highly variable. In particular, the segmentation of the genomic profile must enable to delineate very small regions. Choosing a λ in the AWS procedure, as previously described,¹² equal to the 0.65 quantile of the $\chi^2(1)$ distribution led to an optimal segmentation result. Thresholds of smoothing values were chosen such that early replicating regions account for about 20% of the genome. For the total S phase and S1 fraction of NB cell lines, regions with a smoothing value greater or equal to 1.52 and 1.36, respectively, were considered as early replicating regions, whereas for Sanger's data (lymphoblastoid cell line),¹⁰ we used a threshold of 1.68. To evaluate the proportion of early replicating regions common to both NB cell lines and lymphoblastoid cells in total S phase, we computed the intersection of the early replicating regions defined using the above described procedure between both types of samples.

Correlation between breakpoints' position and replication timing. We compared the distribution of breakpoints in regions of early or late replication. It is necessary to take into account the respective length in bases for each type of regions. Let's assume that the number of breakpoints in regions early and late replicated follows two independent Poisson processes N_E and N_L with parameters λ_E and λ_L . Let's denote L_E and L_L the lengths of the early and late replicating regions, respectively, and x_E and x_L the number of breakpoints in those regions.

The joint distribution is:

$$P(N_E = x_E, N_L = x_L) = \exp(-\mu_E) \mu_E^{x_E} / x_E! \cdot \exp(-\mu_L) \mu_L^{x_L} / x_L!$$

with: $\mu_E = \lambda_E L_E$ and $\mu_L = \lambda_L L_L$

Then the conditional probability is the following:

$$P(N_E = x_E \mid N_E + N_L = x_E + x_L) = C(x_E, x_E + x_L) \theta^{x_L} (1 - \theta)^{x_E}$$

with: $\theta = \mu_E / \mu_E + \mu_L$

The conditional distribution follows a binomial law $B(x_E + x_L, \theta)$ which is used to test the null hypothesis $H_0: \lambda_E = \lambda_L$ with respect to the hypothesis $H_1: \lambda_E \neq \lambda_L$. Under the null hypothesis, $\theta = L_E / L_E + L_L$.

RESULTS

Replication timing of the genome of NB cell lines. We used the microarray replication timing assay recently described¹⁰ to determine the replication timing profile of 7 NB cell lines: CLB-Ge, GI-M-EN, IMR32, KCNR, SJNB-8, SK-N-AS and SK-N-BE. Flow sorted S1 (first quarter of the S phase) or total S phase DNAs labelled with Cy5 were cohybridised with flow sorted G₁ DNA labelled with Cy3. Using this approach, the measured ratio of S/G₁ phase DNAs is, for each clone, a direct measure of the average sequence copy number in the S phase fraction. Chromosome gains or losses, which are identical in the S and G₁ fractions, do not influence this ratio. For each clone, this ratio measures the proportion of nuclei in which this particular sequence has been replicated and hence, evaluates the

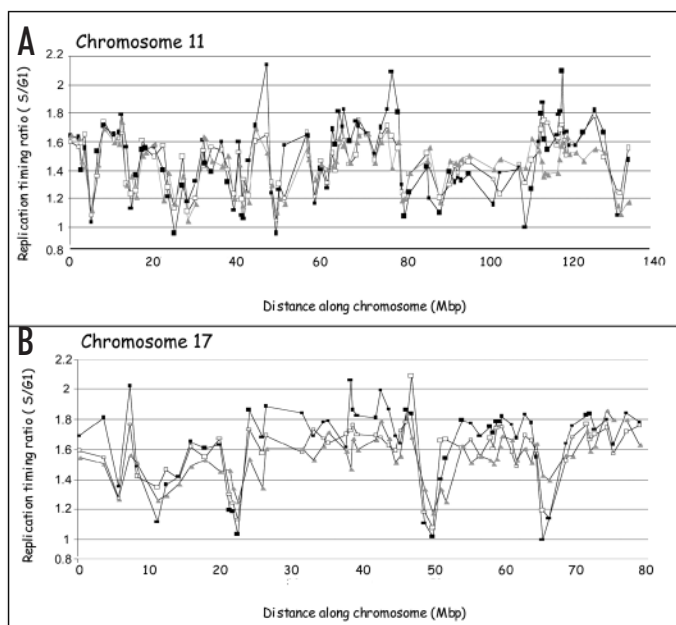


Figure 1. Replication timing profiles of chromosomes 11 and 17 in NB cell lines. DNAs from flow sorted nuclei in G₁ and S phase of the cell cycle were labelled with different fluorochromes and cohybridised on microarrays. Early replicating regions correspond to clones with a S/G₁ ratio close to 2:1. Circles, IMR32; squares, KCNR; triangles, SKNAS.

time at which this sequence replicates. This ratio was further scaled by the value of the median DNA content of the S phase (1.45 for total S, 1.24 for the S1 fraction). Indeed, identical amounts of DNA represent a lower number of S nuclei as compared to G₁ nuclei. Figure 1 shows the replication timing profiles of chromosomes 11 and 17 in three cell lines after sorting and labelling of the total S phase. Complete replication profiles of the seven cell lines are available on the following Web site (<http://microarrays.curie.fr> / Preferential occurrence of chromosome breakpoints within early replicating regions in neuroblastoma / Section 1). Consistent with previous observations, the pattern of replication was not uniform along chromosomes, early replicating regions being clearly interspersed with late replicating regions. Strikingly, the profiles obtained for the different NB cell lines were highly similar: pair-wised correlations of Cy5/Cy3 ratios across the genome for the

analysis of the total S phase DNAs were highly significant (p-values < 10⁻⁴, see Materials and Methods). Similar significances were observed for pair-wised comparisons of S1 fractions. Altogether, these results indicated a general similarity of the temporal replication program in these cell lines.

Given these strong similarities we considered the various NB cell lines as replicates and calculated an average replicating ratio for the seven samples, in total S or S1 fractions (see Materials and Methods). Consistent with previous data, early replicating regions appeared to be more abundant in chromosomes 1, 15, 17, 19 and 22 whereas chromosomes 4, 13, 18, 21 were globally late replicating chromosomes (Fig. 2A). The correlation of Cy5/Cy3 ratios across the genome between S1/G₁ and total S/G₁ fractions was highly significant (r = 0.88 and p < 10⁻⁴) (see chromosome 17 in Fig. 2B). Strong correlations were observed between experiments with directly labelled DNA (total S phase) or with DNA subjected to whole genome amplification prior to labelling (S1 fraction). This indicated that the amplification process does not impair the measurements of the replication timing ratios.

Definition of regions of coordinated replication. In order to more precisely determine regions of coordinate replication, we used the Adaptive Weights Smoothing (AWS) procedure to perform a segmentation analysis on the data averaged from the 7 NB cell lines in total S phase or S1 (see Materials and Methods). Figure 3 shows the segmentation results obtained for chromosomes 11 and 17 using the total S fraction. Chromosome 17 is composed of early replicating segments of large size interspersed with six main segments of late replication (Fig. 3B). The resolution of the array enables to define precisely the borders and size of these segments, respectively of 1.5 Mb, 5.1 Mb, 2.9 Mb, 2.4 Mb, 2.5 Mb and 2.7 Mb. As expected, the six late replicating segments appear to correspond to regions of poor gene content.

We then sought to compare the replication timing profile of the NB cell lines in total S phase to that obtained for a human lymphoblastoid cell line of normal karyotype after a total S phase sorting.¹⁰ In that respect, we obtained, from Kathryn Woodfine and Nigel Carter, the Cy5/Cy3 ratios corresponding to this lymphoblastoid cell line and performed a segmentation analysis of these ratios using the same AWS procedure as for the NB cell lines. The patterns of replication along each chromosome showed a significant level of similarity between the various NB cell lines that have been studied and the lymphoblastoid cell line: indeed, 60% of the early replicating regions defined in NB cell lines appear to be also early replicating in lymphoblastoid cells (<http://microarrays.curie.fr>, Section 2).

Replication timing and position of breakpoints. We then investigated the relationship between the breakpoints' position corresponding to unbalanced translocated chromosomes and the replication profiles in NB cells. Array-CGH profiles for the 27 NB cell lines are available on the Website

(Section 3). Breakpoint positions were determined using the DAGLAD software (Hupé et al manuscript in preparation), a recently modified version of GLAD.¹² A total of 142 breakpoints associated to color transition by 24 color karyotype and gain or loss of genetic material by chromosomal CGH could be further mapped by array-CGH. We investigated the position of these breakpoints with respect to replication timing. Using the replication profile obtained with total S phase, 53.5% of the breakpoints associated to an unbalanced translocation mapped to early

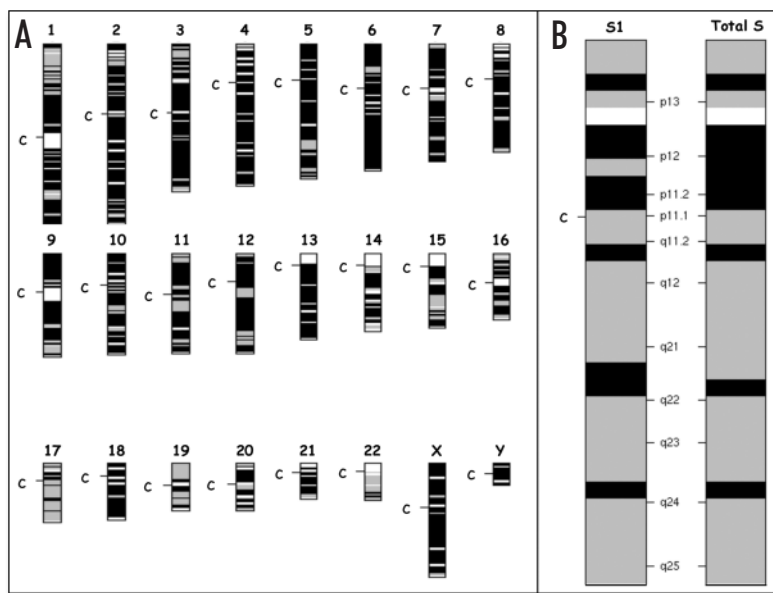


Figure 2. Replication timing pattern of NB cell lines. General view of the mean replication pattern of the whole genome in NB for the early S phase (S1) fraction. For better visualisation, three steps were subsequently applied: (1) for each clone, we calculated a mean replication ratio on the 7 analysed NB cell lines as described in Materials and Methods; (2) the genome was divided into 2.5 Mb intervals and the average ratio for the clones included in each 2.5 Mb interval was calculated, and (3) ratios were colored accordingly: ratio < 1.36, black; ratio > = 1.36, grey; white, not determined. Early replicating regions therefore appear in grey. (B) Expanded views of chromosome 17 for S1 and total S fractions. For total S, ratios were colored accordingly: ratio < 1.52, black; ratio > = 1.52, grey; white, not determined.

replicating regions, which only account for 23.7% of the total genome. These data may be visualized on the Web site (Section 4). Therefore, the breakpoints frequencies per 10^8 bases were 10.84 and 2.94 for early and late replicating regions, respectively. Similarly, using the profiles obtained with the S1 fractions, these breakpoint frequencies were 10.64 and 3.44 for early and late replicating regions, respectively (Table 1). Using the binomial law these differences in breakpoints rate were very highly significant ($p < 10^{-4}$). To rule out a skewed analysis linked to coincidental occurrence of breakpoints and early replicating regions within particular chromosomes, we computed the statistics removing one chromosome at a time. These were still highly significant. Moreover, the p-value computed without the chromosomes 1 and 17 was still strongly significant indicating that the preferential occurrence of breakpoints in early replicating regions is a general characteristic of unbalanced translocations in NB.

DISCUSSION

In this study, we applied the method described by Woodfine et al.¹⁰ to identify early and late replicating regions in NB cells. The power of this assay comes from the use of a genomic microarray and therefore represents a simple genome-wide method to measure the replication profile of a specific cell type. We observed a high similarity between the replication profiles measured for the seven analysed NB cell lines. Moreover, 60% of the early replicating regions defined in NB from the average pattern calculated for the seven samples appear also as regions of early replication in lymphoblastoid cells. These results are in agreement with recently published observations showing that the DNA replication-timing profiles of chromosome 22 is highly similar between different human cells.¹³ Our data further indicate that the bulk of the temporal replication program in human cells is conserved throughout the genome, with differences in particular regions potentially associated to tissue-specific gene regulations.

We then examined the distribution of the breakpoints corresponding to unbalanced translocations in NB cell lines with respect to the replication timing status (early or late). Indeed, previous 24-color karyotyping has suggested that NB translocation breakpoints occur predominantly within early replicating regions.⁶ However, these preliminary experiments were conducted with low resolution cytogenetic methods and did not rely on a specific analysis of the replication timing of NB cells. The present determination of replication profiles and mapping of breakpoints in NB on the same matrix providing a 1 Mb resolution unambiguously show the preferential occurrence of unbalanced translocations in early replicating regions. Further improvement of the resolution may be achieved with arrays containing overlapping tile path clones; indeed, it has been shown recently that a few regions of sharp change in the replication timing profile of chromosome 6 that were not detected at 1 Mb resolution may appear when using a genomic tile path array representing this chromosome.¹⁴

According to their genetic alterations, NB tumors may be classified into two main groups.¹ The first one includes tumors presenting a triploid number of chromosomes, without chromosome rearrangements but only loss or gain of entire chromosomes. The second type contains tumors of near diploid or tetraploid karyotype with unbalanced translocations, which are associated to gain and loss of material of the two implicated chromosomes and characterized by breakpoints arising preferentially outside pericentromeric sites, in early replicating regions. These features distinguish NB from carci-

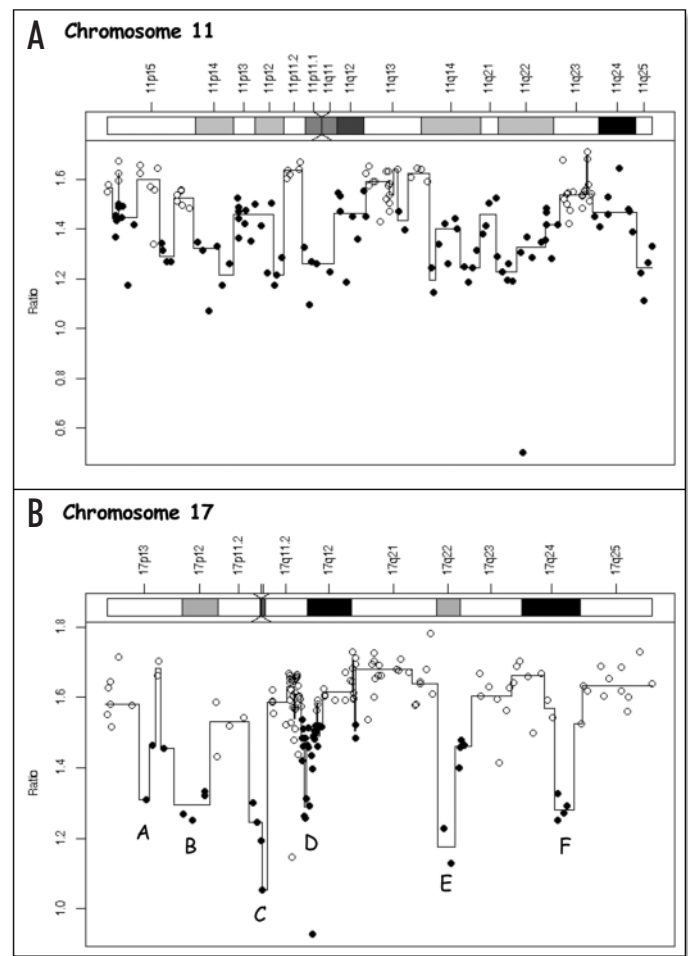


Figure 3. Optimal segmentation for chromosomes 11 and 17 for total S phase. Ratios were colored accordingly: ratio < 1.52 , filled circles; ratio ≥ 1.52 , open circles. See Materials and Methods for details.

nomas. Indeed, recent observations in various carcinomas have suggested that polysomy induces chromosome instability with unbalanced translocations mainly occurring in pericentromeric, late replicating regions.¹⁵ In contrast, terminal and reciprocal (balanced) translocations are more frequent in carcinomas with a near diploid karyotype. Different hypotheses may account for this higher prevalence of translocations breakpoints in early replication regions. The concept that tissue specific chromosomal compartmentalization

Table 1 **Breakpoints associated to unbalanced translocations are preferentially observed in early replicating regions**

	Region length in Mb	Number of BP observed	BP frequency by 10^8 bases
Total S-Early replicating regions	701	76	10.84
Total S-Late replicating regions	2245	66	2.94
S1-Early replicating regions	564	60	10.64
S1-Late replicating regions	2382	82	3.44

A total of 142 breakpoints (BP) characterized by conventional cytogenetic approaches for 27 NB cell lines were further refined using array-CGH. Early and late replicating regions were defined after segmentation analysis of the data obtained for early (S1) or total S phase DNA (see Materials and Methods for details). For each type of region, the BP frequency per 10^8 was calculated according to (Number of BP / Region length in Mb) * 100.

within the nucleus may lead to tumor-specific translocations has recently emerged and is supported by data indicating a physical proximity of chromosomes undergoing translocations.¹⁶ Moreover, the chromosomal compartmentalization seems to be a highly regulated mechanism that preferentially localise early replicating regions in the interior nuclear compartment whereas late replicating regions localize predominantly in the peripheral compartment.¹⁷ Preferential occurrence of 1;17 translocations in NB could therefore rely on a spatial proximity of early replicating donor and recipient chromosomes. Interestingly, early replicating regions mainly correspond to transcriptionally active and gene rich regions, the open chromatin structure of which may favor recombination. In that respect, it has recently been shown in yeast that transcription strongly stimulates mitotic recombination.¹⁸

A model to account for the unbalanced translocations observed in NB is the occurrence of reciprocal translocations between non-homologous chromatids during the S/G₂ phases of the cell cycle, followed by unequal segregation of both derivatives.² In such a model, apart from cases where a selective advantage is provided by one of the derivatives, a random segregation of normal and translocated chromosomes during mitosis should result in the transmission to daughter cells of both derivatives in one fourth of the cases. Such a frequency of reciprocal translocations is much greater than what is observed in NB. An alternative mechanism leading to the accumulation of unbalanced translocations in NB could rely on Break Induced Replication (BIR). In this mechanism, well described in the yeast *Saccharomyces cerevisiae*, the 3' end of a double strand break (DSB) invades a non homologous chromosome and replicates to the telomere, hence leading to an unbalanced translocation.¹⁹ Rad51-dependent and Rad-51-independent BIR mechanisms have been described.^{20,21} During the S phase, DSBs may arise at stalled replication forks and a deficient signalling or repair of these DSBs may serve as a starting point for BIR. Interestingly, interstitial telomere sequences lying at chromosome breakpoints have recently been observed in NB cells, suggesting that a telomere maintenance pathway may be altered in these cells.²² The presence of both unbalanced translocations and telomere insertions suggests that a thorough analysis of the S phase checkpoint may help to understand both replication and telomere abnormalities in NB cells. Finally, a number of studies provided support for a role of segmental duplications in certain chromosome rearrangements.²³⁻²⁵ Sequencing of several breakpoints in NB cell lines may enable this hypothesis to be explored.

Altogether, abnormal signalling of DSBs, nuclear vicinity of heterologous chromosomes, particular chromatin structure of early replicating regions may converge to favor the occurrence of BIR and, hence of unbalanced translocations in NB.

References

1. Brodeur GM. Neuroblastoma: Biological insights into a clinical enigma. *Nat Rev Cancer* 2003; 3:203-16.
2. Caron H, van Sluis P, van Roy N, de Kraker J, Speleman F, Voute PA, Westerveld A, Slater R, Versteeg R. Recurrent 1;17 translocations in human neuroblastoma reveal nonhomologous mitotic recombination during the S/G₂ phase as a novel mechanism for loss of heterozygosity. *Am J Hum Genet* 1994; 55:341-7.
3. Savelyeva L, Corvi R, Schwab M. Translocation involving 1p and 17q is a recurrent genetic alteration of human neuroblastoma cells. *Am J Hum Genet* 1994; 55:334-40.
4. Van Roy N, Laureys G, Van Gele M, Opdenakker G, Miura R, van der Drift P, Chan A, Versteeg R, Speleman F. Analysis of 1;17 translocation breakpoints in neuroblastoma: Implications for mapping of *neuroblastoma* genes. *Eur J Cancer* 1997; 33:1974-8.
5. Van Roy N, Van Limbergen H, Vandesompele J, Van Gele M, Poppe B, Salwen H, Laureys G, Manoel N, De Paep A, Speleman F. Combined M-FISH and CGH analysis allows comprehensive description of genetic alterations in neuroblastoma cell lines. *Genes Chromosomes Cancer* 2001; 32:126-35.
6. Schleiermacher G, Janoueix-Lerosey I, Combaret V, Derre J, Couturier J, Aurias A, Delattre O. Combined 24-color karyotyping and comparative genomic hybridization analysis indicates predominant rearrangements of early replicating chromosome regions in neuroblastoma. *Cancer Genet Cytogenet* 2003; 141:32-42.
7. Schleiermacher G, Peter M, Michon J, Hugot JP, Vielh P, Zucker JM, Magdelenat H, Thomas G, Delattre O. Two distinct deleted regions on the short arm of chromosome 1 in neuroblastoma. *Genes Chromosomes Cancer* 1994; 10:275-81.
8. Trakhtenbrot L, Cohen N, Rosner E, Gipsh N, Brok-Simoni F, Mandel M, Amariglio N, Rechavi G. Coexistence of several unbalanced translocations in a case of neuroblastoma: The contribution of multicolor spectral karyotyping. *Cancer Genet Cytogenet* 1999; 112:119-23.
9. Cohen N, Betts DR, Trakhtenbrot L, Niggli FK, Amariglio N, Brok-Simoni F, Rechavi G, Meitar D. Detection of unidentified chromosome abnormalities in human neuroblastoma by spectral karyotyping (SKY). *Genes Chromosomes Cancer* 2001; 31:201-8.
10. Woodfine K, Fiegler H, Beare DM, Collins JE, McCann OT, Young BD, Debernardi S, Mott R, Dunham I, Carter NP. Replication timing of the human genome. *Hum Mol Genet* 2004; 13:191-202.
11. Fix A, Peter M, Pierron G, Aurias A, Delattre O, Janoueix-Lerosey I. High-resolution mapping of amplicons of the short arm of chromosome 1 in two neuroblastoma tumors by microarray-based comparative genomic hybridization. *Genes Chromosomes Cancer* 2004; 40:266-70.
12. Hupe P, Stransky N, Thierry JP, Radvanyi F, Barillot E. Analysis of array CGH data: From signal ratio to gain and loss of DNA regions. *Bioinformatics* 2004; 20:3413-22.
13. White EJ, Emanuelsson O, Scalzo D, Royce T, Kosak S, Oakeley EJ, Weissman S, Gerstein M, Groudine M, Snyder M, Schubeler D. DNA replication-timing analysis of human chromosome 22 at high resolution and different developmental states. *Proc Natl Acad Sci USA* 2004; 101:17771-6.
14. Woodfine K, Beare DM, Ichimura K, Debernardi S, Mungall AJ, Fiegler H, Collins VP, Carter NP, Dunham I. Replication timing of human chromosome 6. *Cell Cycle* 2005; 4:172-6.
15. Kost-Alimova M, Fedorova L, Yang Y, Klein G, Imreh S. Microcell-mediated chromosome transfer provides evidence that polysomy promotes structural instability in tumor cell chromosomes through asynchronous replication and breakage within late-replicating regions. *Genes Chromosomes Cancer* 2004; 40:316-24.
16. Parada LA, McQueen PG, Misteli T. Tissue-specific spatial organization of genomes. *Genome Biol* 2004; 5:R44.
17. Stein GS, Zaidi SK, Braastad CD, Montecino M, van Wijnen AJ, Choi JY, Stein JL, Lian JB, Javed A. Functional architecture of the nucleus: Organizing the regulatory machinery for gene expression, replication and repair. *Trends Cell Biol* 2003; 13:584-92.
18. Aguilera A. The connection between transcription and genomic instability. *Embo J* 2002; 21:195-201.
19. Cohen N, Ivanov EL, Haber JE. Double-strand break repair in the absence of RAD51 in yeast: A possible role for break-induced DNA replication. *Proc Natl Acad Sci USA* 1996; 93:7131-7136.
20. Davis AP, Symington LS. RAD51-dependent break-induced replication in yeast. *Mol Cell Biol* 2004; 24:2344-51.
21. Ira G, Haber JE. Characterization of RAD51-independent break-induced replication that acts preferentially with short homologous sequences. *Mol Cell Biol* 2002; 22:6384-6392.
22. Schleiermacher G, Bourdeau F, Combaret V, Pierron G, Raynal V, Aurias A, Ribeiro A, Janoueix-Lerosey I, Delattre O. Stepwise occurrence of a complex unbalanced translocation in neuroblastoma leading to insertion of a telomere sequence and late chromosome 17q gain. *Oncogene* 2005; 24:3377-84.
23. Debeer P, Mols R, Huysmans C, Devriendt K, Van de Ven WJ, Fryns JP. Involvement of a palindromic chromosome 22-specific low-copy repeat in a constitutional t(X;22)(q27;q11). *Clin Genet* 2002; 62:410-4.
24. Pujana MA, Nadal M, Guitart M, Armengol L, Gratacos M, Estivill X. Human chromosome 15q11-q14 regions of rearrangements contain clusters of LCR15 duplicons. *Eur J Hum Genet* 2002; 10:26-35.
25. Selzer RR, Richmond TA, Pofahl NJ, Green RD, Eis PS, Nair P, Brothman AR, Stallings RL. Analysis of chromosome breakpoints in neuroblastoma at sub-kilobase resolution using fine-tiling oligonucleotide array CGH. *Genes Chromosomes Cancer* 2005; 44:305-19.